Applied and Computational Mechanics 15 (2021) 45–56

Interaction of a finite crack with shear waves in an infinite magnetoelastic medium

S. K. Panja[a,*], S. C. Mandal[b]

[a]Department of Mathematics, Jadavpur University, Kolkata 700032, West Bengal, India
[b]Faculty of Mathematics, Jadavpur University, Kolkata 700032, West Bengal, India

Received 31 May 2020; accepted 24 May 2021

Abstract

The aim of this paper is to investigate the interaction of a finite crack with shear waves in an infinite magnetoelastic medium. Fourier integral transformation is applied to convert the boundary value problem for a homogeneous, isotropic elastic material to the Fredholm integral equation of second kind. The integral equation is solved by the perturbation method and the effect of magnetic field interaction on the crack is discussed. The stress intensity factor at the crack tip is determined numerically and plotted for low frequencies. Moreover, shear stress outside the crack, crack opening displacement, and crack energy are evaluated and shown by means of graphs.

Keywords: magnetoelastic, finite crack, stress intensity factor, crack opening displacement

1. Introduction

In modern material science, fracture mechanics is an important branch used to refine the performance of mechanical components. Moreover, it covers the study of several laws controlling crack growth. The Griffith theory utters that a crack propagates when the reduction of potential energy due to crack growth crosses over the increase of surface energy due to the formation of a new free surface. This theory is significant for elastic materials. Stress intensity factor (SIF) is one of the most fundamental quantities of crack-related problems. The SIF describes the stress state at the tip of the crack and is used to study failure norm due to fracture. Researchers Robertson [17] and Mal [9–11] have discussed interaction of elastic waves with Griffith cracks in homogeneous infinite elastic medium. Srivastava et al. [18–21] have solved the Griffith/penny shaped crack problems basically located at the interface of two bonded dissimilar elastic half-spaces. Interaction of shear waves with a Griffith crack situated in an infinitely long elastic strip has been studied by Srivastava [22]. Mandal and Mandal [12] have studied the interface crack problem at orthotropic media. Diffraction of P-waves by an edge crack problem within an infinite strip have been discussed by Munshi and Mandal [14] and Aritri et al. [15].

Several decades back a new field of study known as magnetoelasticity emerged, which investigates the relationship between strain and electromagnetic field. Nowadays, magnetoelastic materials are used in high-tech sectors like microwaves, lasers, optics because of their ability to convert one type of energy to another (e.g., mechanical, electrical). In the course of time, magnetoelastic waves are the focal point of research to many research scholars in the field of solid mechanics. A two dimensional diffraction problem of magnetoelastic shear waves by a rigid

*Corresponding author. Tel.: +91 79 80 127 997, e-mail: panjasourav706@gmail.com.
https://doi.org/10.24132/acm.2021.623

strip has been studied by Chattopadhyay and Maugin [5]. Chattopadhyay [3] studied the shear wave propagation problem in a magnetoelastic self-reinforced medium. SH-wave propagation in magnetoelastic orthotropic composite medium was observed by Gupta [8] for multiple layers. Chattopadhyay [6] has given an interesting analysis about crack propagation due to magneto-elastic shear waves in a self-reinforced medium. Chattopadhyay and Bandyopadhyay [2] have also studied the propagation of a crack due to shear waves in a monoclinic type of medium. Furthermore, considering a non-homogeneous medium of monoclinic type, Chattopadhyay et al. [4] have shown the propagation of a crack due to shear waves. Panja and Mandal [16] have discussed the interaction of magnetoelastic shear waves with a Griffith crack within a strip. In the strip problem [16], the nature of SIF is not verified when strip width is infinite, but in the present article, we have examined the magnetoelastic effect in SIF in an infinite medium by an analytical approach. The advantage of the analytical method is that we can plot physical quantities explicitly while in the numerical procedure, discrete data is used to plot SIF.

Even though quite many problems regarding the interaction of crack due to shear waves in an infinite elastic medium have been solved, the problem of interaction of a finite crack with shear waves in an infinite magnetoelastic medium is still unsolved. Therefore, the aim of the present paper is to examine the interaction of a finite crack with shear waves in an infinite magnetoelastic medium by using the perturbation method. The problem has been deduced to the Fredholm integral equation of second kind by means of the Fourier transformation, solution of the integral equation has been derived for low frequencies by the asymptotic series expansion method. To show the effect of magnetoelasticity, SIF has been plotted graphically. Also, variations of other physical parameters like displacement on the crack surface, scattered field, and crack energy have been presented by means of graphs.

2. Problem formulation

Let us assume a Griffith crack of finite width located at $|x_1| \leq l$, $-\infty \leq y_1 \leq \infty$, $z_1 = 0$ in the infinite medium. We normalize all lengths by l and taking $\frac{x_1}{l} = x$, $\frac{y_1}{l} = y$, $\frac{z_1}{l} = z$, the new location of the crack becomes $|x| \leq 1$, $-\infty \leq y \leq \infty$, $z = 0$ symbolized in the Cartesian co-ordinate frame (x, y, z), Fig. 1. We consider a time harmonic incidental shear wave $q_0 e^{-\iota\omega t}$ propagating along the positive z-axis. The term $\mathrm{e}^{-\iota\omega t}$ representing oscillation is common to all field variables and is being suppressed throughout the analysis. The only non-dissipating dimensionless displacement component in the direction of the y-axis is considered to be $u_2 = u_2(x, z)$ as shear waves propagating in the z-direction. ∂_x, ∂_y and ∂_z denote the partial derivatives with respect to x, y and z variables, respectively. Moreover, partial derivatives with

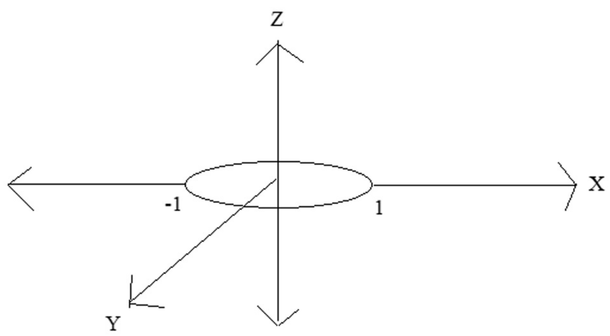

Fig. 1. Configuration of the problem

respect to time t is presented by ∂_t. The governing equations of shear wave propagation in the presence of small elastic disturbances for a absolutely conducting isotropic elastic medium are

$$\partial_x \tau_{xy} + \partial_z \tau_{yz} + (\boldsymbol{J} \times \boldsymbol{B})_y + k^2 u_2 = 0, \tag{1}$$

where $k^2 = \rho\omega^2$ and $(\boldsymbol{J} \times \boldsymbol{B})_y$ is the electromagnetic force ($\boldsymbol{J}$ is the electric current density and $\boldsymbol{B}$ is the magnetic induction vector). The non-zero stress components are

$$\tau_{xy} = \mu \partial_x u_2 \quad \text{and} \quad \tau_{yz} = \mu \partial_z u_2, \tag{2}$$

where coefficient μ is the elastic constant for isotropic medium. The popular Maxwell's equations conducting the electromagnetic field are

$$\boldsymbol{\nabla} \cdot \boldsymbol{B} = 0,\ \boldsymbol{\nabla} \times \boldsymbol{E} = -\partial_t \boldsymbol{B},\ \boldsymbol{\nabla} \times \boldsymbol{H} = \boldsymbol{J},\ \boldsymbol{B} = \mu_e \boldsymbol{H},\ \boldsymbol{J} = \sigma\left(\boldsymbol{E} + \partial_t \boldsymbol{u} \times \boldsymbol{B}\right), \tag{3}$$

where $\boldsymbol{E}$ is the induced electric field, $\boldsymbol{J}$ is the current density vector and the magnetic field $\boldsymbol{H}$ describes both primary and induced magnetic fields. Symbols μ_e and σ are the induced permeability and the conduction coefficient, respectively. The linear Maxwell's stress tensor $\left(\tau_{ij}^0\right)^{M_x}$ due to the magnetic field is given by $\left(\tau_{ij}^0\right)^{M_x} = \mu_e(H_i b_j + H_j b_i - H_k b_k \delta_{ij})$. Let us consider $\boldsymbol{H} = (H_1, H_2, H_3)$ and $b_i = (b_1, b_2, b_3)$, where b_i is the alter in the magnetic field. We have discarded the displacement current. With the help of (3), we write

$$\nabla^2 \boldsymbol{H} = \mu_e \sigma \left[\partial_t \boldsymbol{H} - \boldsymbol{\nabla} \times (\partial_t \boldsymbol{u} \times \boldsymbol{H})\right]. \tag{4}$$

Equation (4) in terms of its components can be written as

$$\begin{aligned} \partial_t H_1 &= \frac{1}{\mu_e \sigma} \nabla^2 H_1, \\ \partial_t H_3 &= \frac{1}{\mu_e \sigma} \nabla^2 H_3, \\ \partial_t H_2 &= \frac{1}{\mu_e \sigma} \nabla^2 H_2 + \partial_x \left(H_1 \partial_t u_2\right) + \partial_z \left(H_3 \partial_t u_2\right). \end{aligned} \tag{5}$$

In absolutely conducting medium (i.e., $\sigma \to \infty$), equations (5) become

$$\partial_t H_1 = \partial_t H_3 = 0 \tag{6}$$

and

$$\partial_t H_2 = \partial_x \left(H_1 \partial_t u_2\right) + \partial_z \left(H_3 \partial_t u_2\right). \tag{7}$$

It is obvious from (6) that H_1 and H_3 have no perturbation. However, equation (7) shows a small perturbation in H_2, say b. Therefore, we have $H_1 = H_1'$, $H_2 = H_2' + b$ and $H_3 = H_3'$, where (H_1', H_2', H_3') are components of the initial magnetic field $\boldsymbol{H'}$. We can write $\boldsymbol{H'} = (H' \cos\theta, 0, H' \sin\theta)$, where $H' = |\boldsymbol{H'}|$ and θ is the angle at which the wave passes the magnetic field. Thus, we have

$$\boldsymbol{H} = (H' \cos\theta, b, H' \sin\theta). \tag{8}$$

We shall take $b = 0$ as the initial value. Substituting (8) in (7), we acquire

$$\partial_t b = \partial_x \left(H' \cos\theta \partial_t u_2\right) + \partial_z \left(H' \sin\theta \partial_t u_2\right). \tag{9}$$

Integrating (9) with respect to t, we have

$$b = H' \cos\theta \partial_x u_2 + H' \sin\theta \partial_z u_2. \tag{10}$$

Keeping in mind $\boldsymbol{\nabla}\left(\frac{H^2}{2}\right) = (\boldsymbol{H}\cdot\boldsymbol{\nabla})\,\boldsymbol{H} - (\boldsymbol{\nabla}\times\boldsymbol{H})\times\boldsymbol{H}$ and taking (3), we get

$$\boldsymbol{J}\times\boldsymbol{B} = \mu_e\left[(\boldsymbol{H}\cdot\boldsymbol{\nabla})\,\boldsymbol{H} - \boldsymbol{\nabla}\left(\frac{H^2}{2}\right)\right]. \tag{11}$$

Substituting the y-component of $\boldsymbol{J}\times\boldsymbol{B}$ in (1), we get the equation of motion in the form

$$P\partial_{xx}u_2 + Q\partial_{zz}u_2 + R\partial_{xz}u_2 + k^2 u_2 = 0, \text{ where } k^2 = \rho\omega^2, \tag{12}$$

and

$$\begin{aligned} P &= \mu + \mu_e H'^2 \cos^2\theta, \\ Q &= \mu + \mu_e H'^2 \sin^2\theta, \\ R &= \mu_e H'^2 \sin 2\theta. \end{aligned} \tag{13}$$

Equation (12) is to be solved with respect to the boundary conditions

$$\tau_{yz}(x,0) = -q_0, \ |x| \le 1 \tag{14}$$

and

$$u_2(x,0) = 0, \ |x| > 1, \tag{15}$$

where q_0 is a known constant. The solution of (12) can be taken as

$$u_2(x,z) = \int_{-\infty}^{\infty} A(u)\mathrm{e}^{-\alpha z}\mathrm{e}^{-\beta z}\mathrm{e}^{\iota u x}\,\mathrm{d}u, \ z > 0, \tag{16}$$

where $\alpha = \frac{\iota u R}{2Q}$ and $\beta = u\sqrt{\frac{1}{Q}\left(P - \frac{k^2}{u^2}\right) - \left(\frac{R}{2Q}\right)^2}$. The non-vanishing stress component is written as

$$\tau_{yz}(x,z) = -\mu\int_{-\infty}^{\infty} (\alpha+\beta)\,A(u)\mathrm{e}^{-\alpha z}\mathrm{e}^{-\beta z}\mathrm{e}^{\iota u x}\,\mathrm{d}u, \tag{17}$$

where $A(u)$ is a unknown function, which is to be determined from the boundary conditions.

3. Derivation of the integral equation

Boundary conditions (14) and (15) lead to the following dual integral equation

$$\int_{-\infty}^{\infty} (\alpha+\beta)\,A(u)\mathrm{e}^{\iota u x}\,\mathrm{d}u = \frac{q_0}{\mu}, \ |x| \le 1 \tag{18}$$

and

$$\int_{-\infty}^{\infty} A(u)\mathrm{e}^{\iota u x}\,\mathrm{d}u = 0, \ |x| > 1. \tag{19}$$

Equation (18) can be written as

$$\int_{-\infty}^{\infty} u\,[1 + H_1(u)]\,A(u)\mathrm{e}^{\iota u x}\,\mathrm{d}u = \frac{q_0}{\gamma\mu}, \ |x| \le 1, \tag{20}$$

where

$$H_1(u) = \frac{H(u)}{\gamma} - 1, \quad H(u) = \frac{\iota R + \sqrt{4Q\left(P - \frac{k^2}{u^2}\right) - R^2}}{2Q},$$
$$\gamma = \frac{\iota R + \sqrt{4QP - R^2}}{2Q}, \quad H_1(u) \to 0 \text{ as } u \to \infty. \tag{21}$$

Let us assume the trial solution of (19) and (20) in the form

$$A(u) = \frac{q_0}{\gamma\mu}\int_0^1 r f(r) J_0(ur)\,\mathrm{d}r \tag{22}$$

so that (19) is trivially satisfied and (20) converts to

$$\int_0^1 r f(r) \int_0^\infty u\left[1 + H_1(u)\right] J_0(ur)\cos(ux)\,\mathrm{d}u\,\mathrm{d}r = 1, \tag{23}$$

where J_0 is the Bessel function of first kind of order zero. Using the Abel's transform in (23) and making simplifications, we find out the following Fredholm integral equation of second kind

$$f(r) + \int_0^1 s f(s)\kappa(s,r)\,\mathrm{d}s = 1, \tag{24}$$

where

$$\kappa(s,r) = \int_0^\infty u H_1(u) J_0(us) J_0(ur)\,\mathrm{d}u. \tag{25}$$

It is notable that the kernel $\kappa(s,r)$ depicted by semi infinite integrals has a slow rate of convergence. Following the procedure of simple contour integration [11], the infinite integral in (25) can be reduced into an integral with finite limits to make the numerical analysis easier. This integral is given by

$$\kappa(s,r) = -\frac{\iota}{2}\int_0^{\frac{k}{\sqrt{P}}} u\frac{\sqrt{R^2 + \frac{4Qk^2}{u^2} - 4PQ}}{Q\gamma} J_0(us) H_0^{(1)}(ur)\,\mathrm{d}u,\ r > s. \tag{26}$$

4. Quantities of physical interest

4.1. Stress intensity factor

Using (17) and (22), we obtain stress components outside the crack in the following form

$$\tau_{yz}(x,0) = q_0\frac{x f(1)}{\sqrt{x^2-1}} + O(1),\ |x| > 1. \tag{27}$$

Defining dimensionless stress intensity factor by

$$K = \lim_{x\to 1^+}\frac{\sqrt{x-1}\,|\tau_{yz}(x,0)|}{q_0},$$

it can be deduced that

$$K = \frac{1}{\sqrt{2}}\,|f(1)|\,. \tag{28}$$

4.2. Crack opening displacement

Another quantity of physical interest is the magnitude of the distance between two edges of the crack, which is given by

$$D(x) = |u_2(x, 0+) - u_2(x, 0-)| = \frac{q_0}{\mu}\left|\int_x^1 \frac{rf(r)}{\sqrt{r^2 - x^2}}\,\mathrm{d}r\right|. \tag{29}$$

For the static case, the value of the distance between two edges of the crack at the centre position of the crack can be written as

$$D_0 = \frac{q_0}{\mu}.$$

Normalizing $D(x)$ with respect to the static displacement between two edges of the crack at the centre position of the crack, we get

$$D = \frac{D(x)}{D_0} = \left|\sqrt{1 - x^2}f(1) - \int_x^1 \sqrt{r^2 - x^2}f'(r)\,\mathrm{d}r\right|, \; |x| < 1. \tag{30}$$

4.3. Crack energy

Crack energy can be calculated as

$$W^* = 2q_0 \int_0^1 u_2(x, 0)\,\mathrm{d}x = 2q_0^2\mu^{-1}\int_0^1 \mathrm{d}x \int_x^1 \frac{r}{\sqrt{r^2 - x^2}}f(r)\,\mathrm{d}r =$$
$$2q_0^2\mu^{-1}\int_0^1 rf(r)\,\mathrm{d}r. \tag{31}$$

The work done by a constant pressure q_0 in opening up a straight Griffith crack is given by

$$W_0 = \frac{q_0^2}{\mu}$$

so that

$$W = \frac{W^*}{W_0} = 2\int_0^1 rf(r)\,\mathrm{d}r. \tag{32}$$

4.4. Scattered field

The shear stress $\tau_{yz}(x, z)$ outside the crack for $x > 1$ and $y > 1$ is calculated from (17) and (22) and has the following form

$$\tau_{yz}(x, z) = -q_0 \int_0^\infty \int_0^1 (\alpha + \beta) rf(r) J_0(ur) \mathrm{e}^{-\alpha z} e^{-\beta z} \cos(ux)\,\mathrm{d}u\,\mathrm{d}r. \tag{33}$$

5. Solution of the integral equation

The iterative solution of the integral equation is derived by the perturbation method with the help of Srivastava et al. [20]. The iterative solution is valid for small values of k. The argument of Bessel functions $J_0(y)$ and $H_0^{(1)}(y)$ is expanded in ascending powers of y as $J_0(y) = \sum_{n=0}^\infty a_{2n}y^{2n}$, $H_0^{(1)}(y) = \left(1 + \frac{2\iota}{\pi}\log\frac{y}{2}\right) J_0(y) + \iota\sum_{n=0}^\infty b_{2n}y^{2n}$, where $a_0 = 1$ and the values of a_{2n} and b_{2n} are given by Abramowitz and Stegun [1]. Using the above expression in (26), $\kappa(s,r)$ can be written as

$$\kappa(s,r) = \left(k^2 \log k\right) \kappa_1(s,r) + \left(k^2\right) \kappa_2(s,r) + \left(k^2 \log k\right)^2 \kappa_3(s,r) + \left(k^4 \log k\right) \kappa_4(s,r) + O\left(k^4\right), \tag{34}$$

where

$$\begin{aligned}
\kappa_1(s,r) &= \frac{M_0}{\pi}, \\
\kappa_2(s,r) &= \frac{N_0}{\pi} + M_0\left(-\frac{\iota}{2} + \frac{b_0}{2} + \frac{1}{\pi}\log\frac{r}{2\sqrt{P}}\right), \\
\kappa_3(s,r) &= 0, \\
\kappa_4(s,r) &= \frac{a_2}{P\pi}\left(s^2 + r^2\right) M_2, \\
M_{2n} &= \int_0^1 \eta_{2n}(u)\,\mathrm{d}u, \\
N_{2n} &= \int_0^1 \eta_{2n}(u)\log(u)\,\mathrm{d}u, \\
\eta_{2n}(u) &= u^{2n}\frac{\sqrt{R^2u^2 + 4PQ(1-u^2)}}{PQ\gamma}.
\end{aligned} \tag{35}$$

Note that $f(s)$ can also be expanded in the form

$$f(s) = f_0(s) + \left(k^2 \log k\right) f_1(s) + \left(k^2\right) f_2(s) + \left(k^2 \log k\right)^2 f_3(s) + \left(k^4 \log k\right) f_4(s) + O\left(k^4\right) \tag{36}$$

and the following terms can be derived

$$\begin{aligned}
f_0(s) &= 1, \\
f_1(s) &= -\frac{M_0}{2\pi}, \\
f_2(s) &= -\frac{N_0}{2\pi} + \frac{M_0}{4}\left(\iota - b_0 + \frac{2}{\pi}\log 2\sqrt{P}\right) + \frac{M_0}{4\pi}\left(1 - s^2\right), \\
f_3(s) &= \left(\frac{M_0}{2\pi}\right)^2, \\
f_4(s) &= \frac{M_0}{\pi}\left[\frac{N_0}{2\pi} + \frac{M_0}{4}\left(b_0 - \iota - \frac{2}{\pi}\log, 2\sqrt{P}\right)\right] - \frac{a_2 M_2}{4P\pi}\left(1 + 2s^2\right) - \left(\frac{M_0}{4\pi}\right)^2\left(3 - 2s^2\right).
\end{aligned} \tag{37}$$

Now, we can easily form $f(s)$ with the help of the aforementioned expression and using (36).

We compare our results with the results of Panja and Mandal [16] by taking $h \to \infty$. The SIF is also derived for a small frequency, i.e., for $k = 0$, and in this case, the problem becomes static in nature. Details are shown in the Appendix.

6. Numerical calculation and discussions

We represent our numerical results graphically for various physical quantities of crack due to shear wave propagation in an infinite magnetoelastic isotropic medium. For the case of isotropic elastic medium, we take the following data [5, 8, 13, 22]:

$$\rho = 2.7\,\mathrm{g/cm^3},\ \mu = \frac{E}{2(1+\eta)},\ \text{ where } \eta = 0.339,\ \ E = 7.05 \times 10^{11}\,\mathrm{dyne/cm^2},$$
$$\epsilon = \frac{\mu_e H'^2}{\mu} = 0.0,\ 0.15,\ 0.30;\ \ \theta = 10°.$$

In Fig. 2, the dimensionless SIF K is plotted against frequency k. The graphs demonstrate the effect of SIF in the presence and absence of magnetoelasticity. For $\epsilon = 0.0$, the curve presents SIF without magnetoelasticity and for $\epsilon = 0.15, 0.30$, the curve shows the nature of SIF in a magnetoelastic isotropic medium. It is noticeable that SIF K decreases after some ascent with increase in frequency k for each instance. The decreasing nature of SIF with the increase in frequency k are similar to the results presented by Panja and Mandal [16]. In the present work, the solution procedure is valid for low frequencies, therefore, the decreasing rate of SIF is slightly slower in an infinite medium than in a strip. Although within $k \leq 2.5$, the SIF curves obtained in this paper are in agreement with the results examined in [16]. The current paper also confirms that SIF decreases with an increase in strip width ([16]) as SIF in an infinite medium starts from 0.7, compared to the case of a finite width strip, where SIF starts from higher values than 0.7 for the same material. In the magnetoelastic medium, the decrement rate of SIF is less than isotropic elastic media.

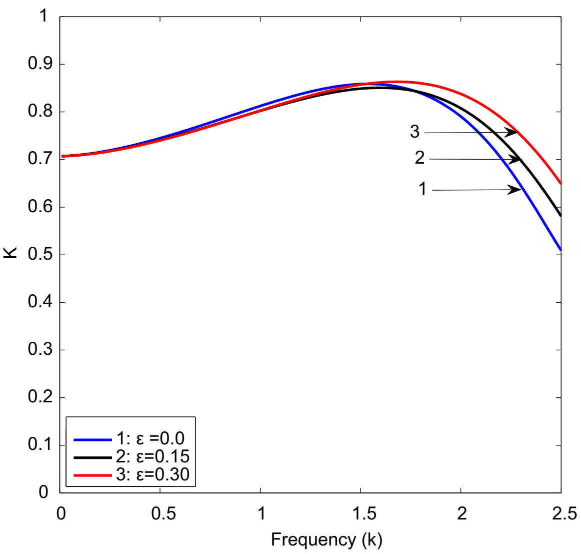

Fig. 2. SIF K against dimensionless frequency k

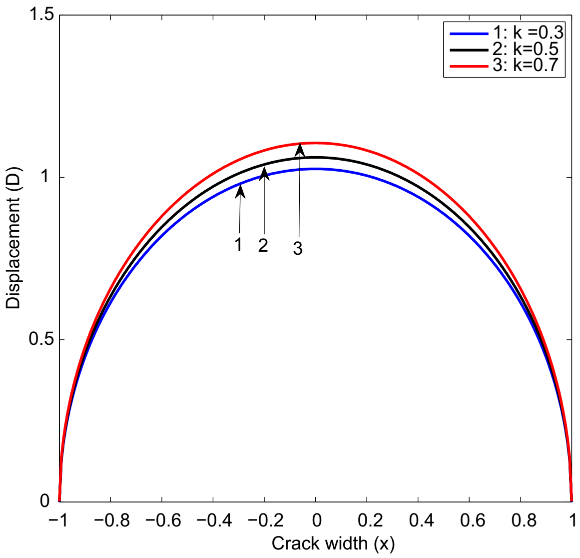

Fig. 3. Displacement D against crack width x

Fig. 3 shows the plot of crack opening displacement (COD) D versus crack width x in the absence of magnetoelasticity, i.e., $\epsilon = 0$ for different values of frequency. It is notable that the graph is symmetric about $x = 0$, the COD achieves its highest value at point $x = 0$ and reaches a zero value at the tips of the cracks. The COD increases gradually for higher values of frequency k. The change of graphs is insignificant for the magnetoelastic effect.

In Fig. 4, we have plotted the graph of crack energy W versus frequency k. The nature of this graph is quite similar to the graph of SIF versus frequency k (Fig. 2). Only one thing is noticeable, namely, the crack energy W has a rather lower decrement rate with increasing frequency than the SIF.

Fig. 5 is the surface plot of shear stress just outside the crack for $k = 0.3$ in the absence of magnetoelasticity. Fig. 6 shows the nature of scattered field in the magnetoelastic medium for $k = 0.3$. It has been noticed that the dimensionless scattered field behaves like a wave and looses sharpness with an increase in the z-direction.

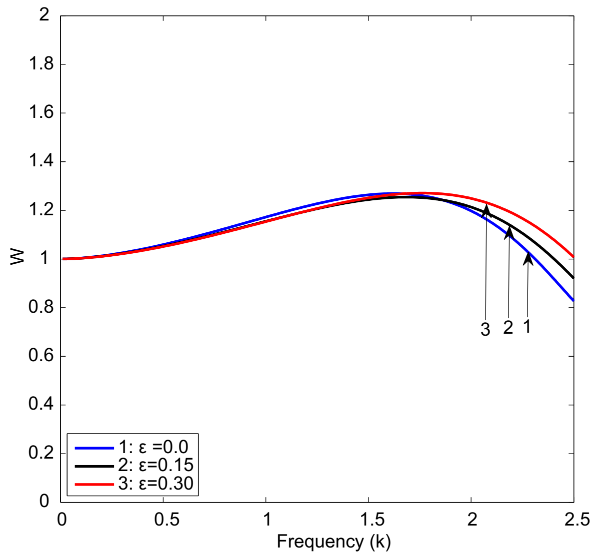

Fig. 4. Crack energy W against dimensionless frequency k

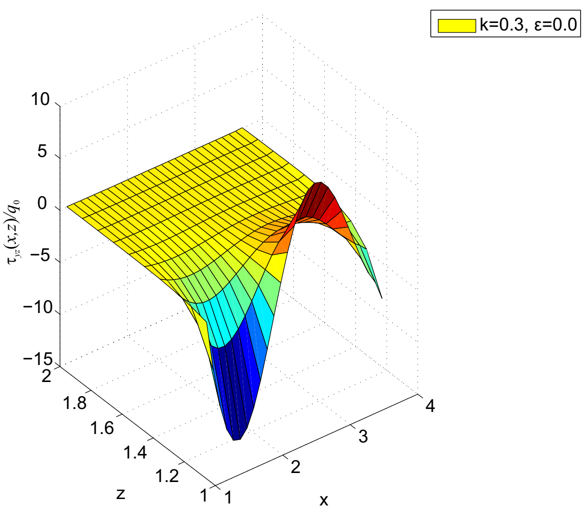

Fig. 5. Scattered field outside the crack in the absence of magnetoelasticity

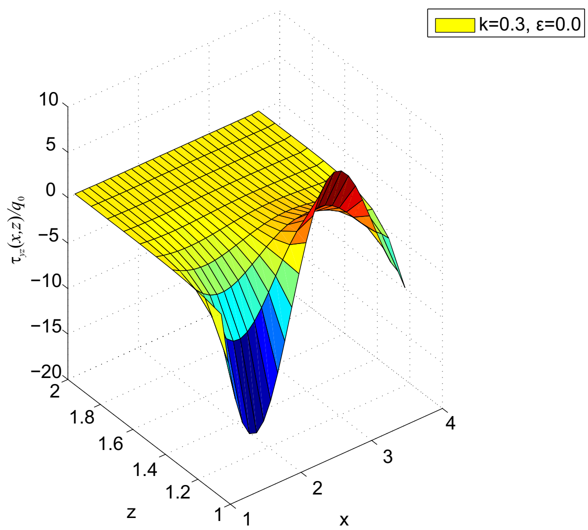

Fig. 6. Scattered field outside the crack in a magnetoelastic medium

7. Conclusion

An analytical method for studying the effect of magnetoelasticity on the stress intensity factor (SIF) of a finite crack in an infinite elastic medium was introduced. This analytical method to solve the Fredholm integral equation of second kind is very straightforward and easy to compute compared to the numerical procedure, which is very laborious and time-consuming. We derived some physical quantities such as SIF, crack opening displacement, crack energy, and scattered field, which were plotted graphically. The following lists the outcomes of this study:

- Crack growth is more influential in a magnetoelastic medium than in a non-magnetoelastic medium for low frequencies. Crack energy carries out the same effect for the magnetic field.
- Fracture loses its toughness for higher values of frequency.
- In the neighborhood of the crack, the non-dimensionless stress component is very disruptive in nature and loses its divisiveness far away from the crack.

This paper is useful for small cracks. An extension of the concept for large deformations is very difficult. Nevertheless, this research outcome may be very significant for the study of fracture toughness, crack tip opening displacement and crack growth controlling development features in the field of fabrication processes in fracture mechanics. Further extended models, for example, for two or three linear cracks in a composite material, using different mediums, and interfaced crack problems in the presence of magnetoelasticity can be studied with the help of the present work.

Acknowledgements

This research work is developed with the financial help of RUSA 2.0, Jadavpur University, Kolkata-700032.

References

[1] Abramowitz, M., Stegun, I. A., Handbook of mathematical functions with formulas, graphs, and mathematical tables, Vol. 55, US Government printing office, US, 1948.

[2] Chattopadhyay, A., Bandyopadhyay, U., Propagation of a crack due to shear waves in a medium of monoclinic type, Acta Mechanica 71 (1–4) (1988) 145–156. https://doi.org/10.1007/BF01173943

[3] Chattopadhyay, A., Gupta, S., Singh, A. K., The dispersion of shear wave in multilayered magnetoelastic self-reinforced media, International Journal of Solids and Structures 47 (9) (2010) 1317–1324. https://doi.org/10.1016/j.ijsolstr.2010.01.019

[4] Chattopadhyay, A., Keshri, A., Choudhury, S., Propagation of a crack due to shear waves in a non-homogeneous medium of monoclinic type, Indian Journal of Pure and Applied Mathematics 25 (11) (1994) 1195–1205.

[5] Chattopadhyay, A., Maugin, G. A. Diffraction of magnetoelastic shear waves by a rigid strip, The Journal of the Acoustical Society of America 78 (1) (1985) 217–222. https://doi.org/10.1121/1.392561

[6] Chattopadhyay, A., Singh, A. K., Propagation of a crack due to magnetoelastic shear waves in a self-reinforced medium, Journal of Vibration and Control 20 (3) (2014) 406–420. https://doi.org/10.1177/1077546312458134

[7] Fox, L., Goodwin, E. T., The numerical solution of non-singular linear integral equations, Philosophical Transactions of the Royal Society of London, Series A, Mathematical and Physical Sciences 245 (902) (1953) 501–534. https://doi.org/10.1098/rsta.1953.0005

[8] Gupta, S., Bhengra, N., Implementation of finite difference approximation on the SH-wave propagation in a multilayered magnetoelastic orthotropic composite medium, Acta Mechanica 228 (10) (2017) 3421–3444. https://doi.org/10.1007/s00707-017-1884-6

[9] Mal, A. K., Dynamic stress intensity factor for an axisymmetric loading of the penny shaped crack, International Journal of Engineering Science 6 (11) (1968) 623–629. https://doi.org/10.1016/0020-7225(68)90063-3

[10] Mal, A. K., Dynamic stress intensity factor for a non-axisymmetric loading of the penny shaped crack, International Journal of Engineering Science 6 (12) (1968) 725–733. https://doi.org/10.1016/0020-7225(68)90010-4

[11] Mal, A. K., Interaction of elastic waves with a Griffith crack, International Journal of Engineering Science 8 (9) (1970) 763–776. https://doi.org/10.1016/0020-7225(70)90003-0

[12] Mandal, P., Mandal, S. C., Interface crack at orthotropic media, International Journal of Applied and Computational Mathematics 3 (4) (2017) 3253–3262. https://doi.org/10.1007/s40819-016-0290-4

[13] Maugin, G. A., Wave motion in magnetizable deformable solids, International Journal of Engineering Science 19 (3) (1981) 321–388. https://doi.org/10.1016/0020-7225(81)90059-8
[14] Munshi, N., Mandal, S. C., Diffraction of P-waves by edge crack in an infinitely long elastic strip, JSME International Journal Series A Solid Mechanics and Material Engineering 49 (1) (2006) 116–122. https://doi.org/10.1299/jsmea.49.116
[15] Nandi, A., Basak, P., Mandal, S. C., Diffraction of p-waves by edge crack in an infinite orthotropic strip, International Journal of Applied and Computational Mathematics 1 (4) (2015) 543–557. https://doi.org/10.1007/s40819-015-0028-8
[16] Panja, S. K., Mandal, S. C., Interaction of magnetoelastic shear waves with a Griffith crack in an infinite strip, Journal of Engineering Mathematics 126 (1) (2021) 1–11. https://doi.org/10.1007/s10665-020-10085-0
[17] Robertson, I. A., Diffraction of a plane longitudinal wave by a penny-shaped crack, Mathematical Proceedings of the Cambridge Philosophical Society 63 (1), Cambridge University Press, 1967. https://doi.org/10.1017/S0305004100041116
[18] Srivastava, K. N., Gupta, O. P., Palaiya, R. M., Interaction of elastic waves in two bonded dissimilar elastic half-planes having Griffith crack at interface-I, International Journal of Fracture 14 (2) (1978) 145–154. https://doi.org/10.1007/BF00032541
[19] Srivastava, K. N., Palaiya, R. M., Gupta, O. P., Interaction of longitudinal wave with a pennyshaped crack at the interface of two bonded dissimilar elastic solids-II, International Journal of Fracture 15 (6) (1979) 591–599. https://doi.org/10.1007/BF00019925
[20] Srivastava, K. N., Palaiya, R. M., Karaulia, D. S., Interaction of antiplane shear waves by a Griffith crack at the interface of two bonded dissimilar elastic half-spaces, International Journal of Fracture 16 (4) (1980) 349–358. https://doi.org/10.1007/BF00018239
[21] Srivastava, K. N., Palaiya, R. M., Karaulia, R. M., Diffraction of SH waves by two coplanar Griffith cracks at the interface of two bonded dissimilar elastic half-spaces, Indian Journal of Pure and Applied Mathematics 12 (2) (1981) 242–252.
[22] Srivastava, K. N., Palaiya, R. M., Karaulia, D. S., Interaction of shear waves with a Griffith crack situated in an infinitely long elastic strip, International Journal of Fracture 21 (1) (1983) 39–48. https://doi.org/10.1007/BF01134198

Appendix

Making the strip width infinite, i.e., $h \to \infty$, the integral equation (41) in the paper Panja and Mandal [16] becomes

$$g(t) + \int_0^1 ug(u)L_1(u,t)\,\mathrm{d}u = 1,$$

which is similar to the integral equation (24) in the present paper as the kernel

$$L_2(u,t) = \imath k_1^2 \int_0^1 \sqrt{1-y^2} J_0(k_1yt)J_0(k_1yu)\csc(k_1yh)\mathrm{e}^{-k_1yh}\,\mathrm{d}y - \imath k_1^2 \int_0^\infty \sqrt{1+y^2} I_0(k_1yt)I_0(k_1yu)\frac{\mathrm{e}^{-k_1yh}}{\sinh(k_1yh)}\,\mathrm{d}y$$

in the published paper [16] vanishes for $h \to \infty$. The nature of the SIF in the present article approaches the result obtained by Panja and Mandal [16] for a crack in a strip when the strip width becomes very large.

For the frequency $k = 0.0$, the current dynamic problem becomes static in nature and kernel $\kappa(s,r)$ disappears, which implies $f(r) = 1$ and SIF $K = \frac{1}{\sqrt{2}} = 0.71$, i.e., exactly the same as presented by the graph shown above.

In Fig. 7, the values of SIF are compared between iterative and numerical solutions. Curve 1 represents the SIF derived numerically by the mehod of Fox and Goodwin [7], used in the paper [16], whereas curve 2 presents the SIF values obtained analytically by the perturbation method. Because the two curves have a very similar nature for values of frequency $k < 2.5$, we can say that the iterative solution given by (36) projects reasonably accurate result of SIF in the range $0 < k < 2.5$.

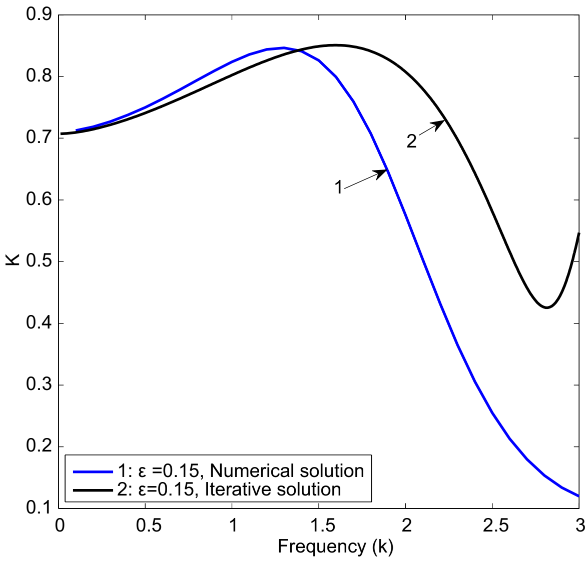

Fig. 7. Comparison between numerical and iterative solution of SIF